Magnon Spin Nernst Effect in Antiferromagnets

Vladimir A. Zyuzin and Alexey A. Kovalev

Phys. Rev. Lett. **117**, 217203 — Published 15 November 2016

DOI: 10.1103/PhysRevLett.117.217203

Magnon spin Nernst effect in antiferromagnets

Vladimir A. Zyuzin[1] and Alexey A. Kovalev[1]

[1] *Department of Physics and Astronomy and Nebraska Center for Materials and Nanoscience, University of Nebraska, Lincoln, Nebraska 68588, USA*

We predict that a temperature gradient can induce a magnon-mediated spin Hall response in an antiferromagnet with non-trivial magnon Berry curvature. We develop a linear response theory which gives a general condition for a Hall current to be well defined, even when the thermal Hall response is forbidden by symmetry. We apply our theory to a honeycomb lattice antiferromagnet and discuss a role of magnon edge states in a finite geometry.

Understanding spin transport in nanostructures is a long-standing problem in the field of spintronics [1–3]. The discovery of the spin Hall effect [4–10] has been extremely important as it has led to many important developments in spintronics [11], such as the quantum spin Hall effect [12, 13], the spin-orbit torque [14–16], and the spin Seebeck effect [17–19]. In the instrinsic spin Hall effect, the time reversal symmetry prohibits the transverse charge current but allows the transverse spin current originating from the non-trivial Berry curvature of electron bands [7, 8]. The quantization of the intrinsic spin Hall effect can be characterized by the topological Chern number and is accompanied by the existence of topologically protected edges in the finite geometry [20]. On the other hand the quantum spin Hall effect can be characterized by the Z2 topological invariant [12, 13].

The thermal Hall effect carried by magnons has been experimentally observed in collinear ferromagnets such as $Lu_2V_2O_7$, $Ho_2V_2O_7$, and $In_2Mn_2O_7$ with pyrochlore structure [21, 22]. It has been understood that the Dzyaloshinskii-Moriya interaction (DMI) leads to the Berry curvature of magnon bands and to the transverse with respect to the external temperature gradient energy current [23–26]. The same effect has also been observed in kagome ferromagnet $Cu(1-3, bdc)$ [27]. The existence of magnon edge states and tunable topology of magnon bands have been discussed theoretically [24, 25, 28–31]. The spin Nernst effect (SNE) has been theoretically studied in Ref. [32] for a kagome lattice ferromagnet. Topological properties of honeycomb lattice ferromagnet were addressed in Refs. [33–35].

It has been recently realized that antiferromagnets are promising materials for spintronics applications [36]. In Refs. [37, 38] the spin Seebeck effect has been studied in antiferromagnets. In Ref. [39] it has been shown that the Berry curvature can result in non-zero thermal Hall effect carried by magnons in magnets with dipolar interaction and in antiferromagnets. However, SNE in antiferromagnets has not been addressed as all of the studies of anomalous magnon-mediated spin transport in magnetic materials have so far been done in ferromagnetic systems.

In this paper, we study SNE in antiferromagnets with Neel order. We first derive a general operator that has a well defined current in a general antiferromagnet. We then develop a linear response theory for such a current using the Luttinger approach of the gravitational scalar potential [40, 41]. It is shown that the response is driven by a modified Berry curvature of magnon bands. We then apply our findings to antiferromagnets with Neel order where a well defined current corresponds to the spin density. Various realizations of antiferromagnets with honeycomb arrangement of magnetic atoms have been suggested recently [42–46]. We consider a single- and bi-layer honeycomb antiferromagnets with antiferromagnetic interlayer coupling where the nearest neighbor exchange interactions and the second nearest neighbor DMI are present (see Fig. 1). We show that both models possess the magnon edge states in the finite geometry and discuss their role for SNE. For a single layer, we observe an interplay between the Berry curvature due to the lattice topology and DMI and find that the Berry curvature is not of the monopole type, contrary to a ferromagnet on a honeycomb lattice [34, 35]. We also find that SNE can be present in antiferromagnets that are invariant under (i) a global time reversal symmetry (e.g. Fig. 1, right) or under (ii) a combined operation of time reversal and inversion symmetries (e.g. Fig. 1, left) which prohibits the thermal Hall response derived in [39].

Current in antiferromagnet. Here we assume a general model of antiferromagnet insulator with a magnetic unit cell having N sites. The Hamiltonian of such a system is of Heisenberg type with exchange interactions, DMI, anisotropies and others. Assuming that we know the order of the system, we study the magnon excitations around that order. The Holstein-Primakoff transformation from spins to boson operators can be employed to study the magnons (see [47] for example). In this way, the boson operators $\nu_j(\mathbf{r})$ and $\nu_j^\dagger(\mathbf{r})$, with $j \in (1, N)$, correspond to jth element of the magnetic unit cell. The operators satisfy commutation relationship $[\nu_i(\mathbf{r}), \nu_j^\dagger(\mathbf{r}')] = \delta_{ij}\delta_{\mathbf{r}\mathbf{r}'}$. We then proceed to write a general form of a Hamiltonian describing the magnons,

$$H_0 = \frac{1}{2}\int d\mathbf{r}\Psi^\dagger(\mathbf{r})\hat{H}\Psi(\mathbf{r}). \quad (1)$$

Since this Hamiltonian describes magnons of an antiferromagnet, it will necessary contain pairing terms of

boson operators. One must then extend the space of the Hamiltonian, such that the spinor $\Psi(\mathbf{r})$ is written as $\Psi(\mathbf{r}) = [\nu_1(\mathbf{r}), ..., \nu_N(\mathbf{r}), \nu_1^\dagger(\mathbf{r}), ..., \nu_N^\dagger(\mathbf{r})]^{\mathrm{T}}$.

The Hamiltonian in $\mathbf{k}-$space can be diagonalized with a help of a paraunitry matrix $T_\mathbf{k}$, such that

$$T_\mathbf{k}^\dagger \hat{H}_\mathbf{k} T_\mathbf{k} = \varepsilon_\mathbf{k} = \begin{bmatrix} E_\mathbf{k} & 0 \\ 0 & E_{-\mathbf{k}} \end{bmatrix}, \tag{2}$$

where $E_\mathbf{k}$ is a $N \times N$ diagonal matrix of eigenvalues. Paraunitarity of the matrix $T_\mathbf{k}$ means that it has to satisfy a condition $T_\mathbf{k}^\dagger \sigma_3 T_\mathbf{k} = \sigma_3$.

We will be interested in responses of the system to external temperature gradient. To treat the temperature gradient we adopt the Luttinger model [40] and add gravitational potentials to the Hamiltonian as

$$H = \frac{1}{2}\int d\mathbf{r} \tilde{\Psi}^\dagger(\mathbf{r}) \hat{H} \tilde{\Psi}(\mathbf{r}), \tag{3}$$

where $\tilde{\Psi}(\mathbf{r}) = \left(1 + \frac{\mathbf{r}\boldsymbol{\nabla}\chi}{2}\right)\Psi(\mathbf{r})$ with $\boldsymbol{\nabla}\chi$ being the temperature gradient with $\chi(\mathbf{r}) = -T(\mathbf{r})/T$.

Let us now introduce an arbitrary operator $\hat{O}$ acting in the Hilbert space of the studied system. Density of such an operator is $\mathcal{O}(\mathbf{r}) = \frac{1}{2}\Psi^\dagger(\mathbf{r})\hat{O}\Psi(\mathbf{r})$. Time evolution of the density is derived through a commutator with total Hamiltonian as, see Supplemental Material (SM) for details, follows

$$\begin{aligned} \frac{\partial \mathcal{O}(\mathbf{r})}{\partial t} &= i[H, \mathcal{O}(\mathbf{r})] \\ &= -\frac{1}{2}\boldsymbol{\nabla}\tilde{\Psi}^\dagger(\mathbf{r})\left(\hat{\mathbf{v}}\sigma_3\hat{O} + \hat{O}\sigma_3\hat{\mathbf{v}}\right)\tilde{\Psi}(\mathbf{r}) \\ &- i\frac{1}{2}\tilde{\Psi}^\dagger(\mathbf{r})\left(\hat{O}\sigma_3\hat{H} - \hat{H}\sigma_3\hat{O}\right)\tilde{\Psi}(\mathbf{r}), \end{aligned} \tag{4}$$

where $\hat{\mathbf{v}} = i[\hat{H}, \mathbf{r}]$ is the velocity operator, and σ_3 is the third Pauli matrix operating in the extended space of the Hamiltonian (1). In deriving we assumed that the operator $\hat{O}$ commutes with the position operator. From (4) we observe that for the current of an operator $\hat{O}$ to be well defined, a

$$\hat{O}\sigma_3\hat{H} - \hat{H}\sigma_3\hat{O} = 0 \tag{5}$$

condition must be satisfied by the operator $\hat{O}$. Otherwise the quantity associated with the density $\mathcal{O}(\mathbf{r})$ will not be conserved in our system. Let us assume we have found such an operator that satisfies the condition (5), the current associated with this operator is then defined as

$$\mathbf{j}_\mathrm{O}(\mathbf{r}) = \tilde{\Psi}^\dagger(\mathbf{r})\hat{O}\sigma_3\hat{\mathbf{v}}\tilde{\Psi}(\mathbf{r}). \tag{6}$$

Let us now calculate the response of the $\hat{O}-$operator current to the temperature gradient. We will be working with the macroscopic currents, defined as $\mathbf{J}_\mathrm{O} = \frac{1}{V}\int d\mathbf{r}\mathbf{j}_\mathrm{O}(\mathbf{r})$, where V is volume of the system. Note that the current consists of unperturbed part $\mathbf{J}_\mathrm{O}^{[0]} = \frac{1}{V}\int d\mathbf{r}\Psi^\dagger(\mathbf{r})\hat{O}\sigma_3\mathbf{v}\Psi(\mathbf{r})$ and a perturbed by a temperature gradient $\mathbf{J}_\mathrm{O}^{[1]} = \frac{1}{2V}\int d\mathbf{r}\Psi^\dagger(\mathbf{r})\hat{O}\sigma_3\left(r_\beta\hat{\mathbf{v}} + \hat{\mathbf{v}}r_\beta\right)\Psi(\mathbf{r})\nabla_\beta\chi$ part. Both of them must be used to calculate linear response to the temperature gradient. The total current is

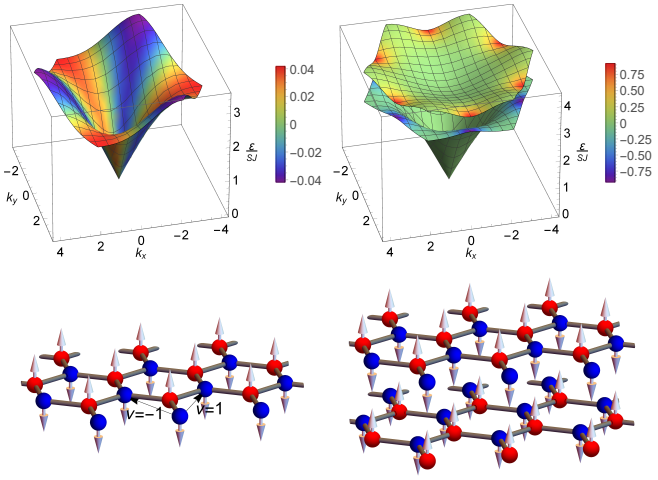

FIG. 1. (Color online) Left: Magnon spectrum of a single layer antiferromagnet with DMI $D = 0.1J$ (black arrows correspond to ν sign convention of DMI), with schematics of the lattice and order in $z-$direction in the bottom. Right: Magnon spectrum of antiferromagnet on a bilayer honeycomb lattice. Parameters are chosen to be $J' = J$ and $D = 0.1J$. In both cases the distribution of the Berry curvature over the Brillouin zone is plotted by the color distribution on top of the spectrum for one of the degenerate subbands.

$$\mathbf{J}_\mathrm{O} = \left\langle \mathbf{J}_\mathrm{O}^{[0]} \right\rangle_\mathrm{ne} + \left\langle \mathbf{J}_\mathrm{O}^{[1]} \right\rangle_\mathrm{eq}. \tag{7}$$

The first term is evaluated with respect to nonequilibrium states and can be conveniently captured by the Kubo linear response formalism. Second current corresponds to magnetization in the system and it is evaluated with respect to equilibrium state. To calculate the latter, we adopt Smrcka and Streda approach [48] and adopt derivations presented in [39]. It is important to note that the velocity written in the diagonal basis as $\tilde{v}_{\alpha\mathbf{k}} = T_\mathbf{k}^\dagger \hat{v}_\alpha T_\mathbf{k} = \partial_\alpha\varepsilon_\mathbf{k} + \mathcal{A}_{\alpha\mathbf{k}}\sigma_3\varepsilon_\mathbf{k} - \varepsilon_\mathbf{k}\sigma_3\mathcal{A}_{\alpha\mathbf{k}}$, is conveniently separated into diagonal and non-diagonal parts, where $\mathcal{A}_{\alpha\mathbf{k}} = T_\mathbf{k}^\dagger\sigma_3\partial_\alpha T_\mathbf{k}$. The latter is responsible for the transverse responses of the system. The details of the calculations for the current are given in SM. Overall, the total current is derived to be

$$[\mathbf{J}_\mathrm{O}]_\alpha = \frac{1}{V}\sum_{\mathbf{k}n}[\bar{\Omega}_{\alpha\beta}^{[\mathrm{O}]}(\mathbf{k})]_{nn} c_1\left[(\sigma_3\varepsilon_\mathbf{k})_{nn}\right]\nabla_\beta\chi, \tag{8}$$

where $c_1(x) = \int_0^x d\eta\ \eta\frac{dg(\eta)}{d\eta}$, and $g(\eta) = (e^{\eta/T} - 1)^{-1}$ is the Bose-Einstein distribution function. We defined an

O−Berry curvature,

$$\bar{\Omega}^{[\mathrm{O}]}_{\alpha\beta}(\mathbf{k}) = i\bar{O}\partial_\alpha T^\dagger_{\mathbf{k}}\sigma_3\partial_\beta T_{\mathbf{k}} - (\alpha \leftrightarrow \beta)\,, \qquad (9)$$

a Berry curvature modified with an operator $\bar{O} = \sigma_3 T^\dagger_{\mathbf{k}}\hat{O}T_{\mathbf{k}}\sigma_3$. Due to commutation relations (5), matrix $\bar{O}$ is diagonal in band index. We show there is a sum rule $\sum_n[\bar{\Omega}^{[\mathrm{O}]}_{\alpha\beta}(\mathbf{k})]_{nn} = 0$ the O−Berry curvature satisfies. Expressions (8) and (9) together with (5) and (6) are the main results of this paper.

Single layer honeycomb antiferromagnet. We now apply our results to specific model of an antiferromagnet on honeycomb lattice. The lattice of the system is shown in Fig. 1. We define an exchange Hamiltonian

$$H = J\sum_{<ij>}\mathbf{S}_i\mathbf{S}_j + D\sum_{<<ij>>}\nu_{ij}\left[\mathbf{S}_i\times\mathbf{S}_j\right]_z. \qquad (10)$$

Here $J>0$ is the nearest neighbor spin exchange, D is the strength of the second-nearest neighbor spin DMI, and ν_{ij} is a sign convention defined in Fig. 1.

Let us assume there is a Neel order in the direction perpendicular to lattice plane, z−direction. To study magnons of the model we perform Holstein-Primakoff transformation from spins to boson operators, $S_{A+} = \sqrt{2S-a^\dagger a}a$, $S_{Az} = S - a^\dagger a$, and $S_{B+} = -\sqrt{2S-b^\dagger b}b^\dagger$, $S_{Bz} = -S + b^\dagger b$, and assume large S limit. As shown in SM, the Hamiltonian describing non-interacting magnons splits in to two blocks. The first block, call it I, is described by $\Psi_{\mathrm{I}} = (a_{\mathbf{k}}, b^\dagger_{-\mathbf{k}})^{\mathrm{T}}$ spinor. The Fourier image of the Hamiltonian of the first block is

$$H_{\mathrm{I}\mathbf{k}} = JS\begin{bmatrix} 3+\Delta_{\mathbf{k}} & -\gamma_{\mathbf{k}} \\ -\gamma_{-\mathbf{k}} & 3-\Delta_{\mathbf{k}}\end{bmatrix}. \qquad (11)$$

where we defined $\gamma_{\mathbf{k}} = 2e^{i\frac{k_x}{2\sqrt{3}}}\cos(\frac{k_y}{2}) + e^{-i\frac{k_x}{\sqrt{3}}}$, and $\Delta_{\mathbf{k}} = 2\frac{D}{J}[\sin(k_y) - 2\sin(\frac{k_y}{2})\cos(\frac{\sqrt{3}k_x}{2})]$ is the DMI, and we note $\Delta_{\mathbf{k}} = -\Delta_{-\mathbf{k}}$. Hamiltonian of the second block described by $\Psi_{\mathrm{II}} = (b_{\mathbf{k}}, a^\dagger_{-\mathbf{k}})^{\mathrm{T}}$ spinor is obtained by $\gamma_{\mathbf{k}} \to \gamma_{-\mathbf{k}}$ in (11).

Let us define operator $\hat{O}$ acting in full, $\Psi_{\mathbf{k}} = (a_{\mathbf{k}}, b_{\mathbf{k}}, a^\dagger_{-\mathbf{k}}, b^\dagger_{-\mathbf{k}})^{\mathrm{T}}$, space as

$$\hat{O} = \begin{bmatrix}\hat{\tau}_3 & 0\\ 0 & \hat{\tau}_3\end{bmatrix}, \qquad (12)$$

where $\hat{\tau}_3$ is third 2×2 Pauli matrix. The density of this operator written in real space, $\mathcal{O}(\mathbf{r}) = \frac{1}{2}\Psi^\dagger(\mathbf{r})\hat{O}\Psi(\mathbf{r}) = a^\dagger(\mathbf{r})a(\mathbf{r}) - b^\dagger(\mathbf{r})b(\mathbf{r})$, is the spin density. It can be shown that such an operator satisfies condition (5), thus the spin density current associated with $\hat{O}$ is well defined. Let us now calculate the spin density current as a response to the temperature gradient. Expression for the response is given by (8), hence we need to find eigenvalues and calculate O−Berry curvature.

Spectrum of magnons for both blocks of the Hamiltonian is obtained to be

$$E_{\mathbf{k}} = JS\left(\Delta_{\mathbf{k}} + \sqrt{9-|\gamma_{\mathbf{k}}|^2}\right). \qquad (13)$$

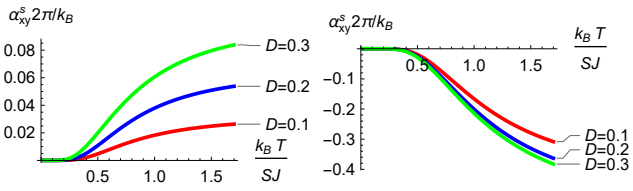

FIG. 2. (Color online) Spin Nernst conductivity α^{s}_{xy}, defined after expression (15). Left: a single layer honeycomb antiferromagnet. Right: double layer honeycomb antiferromagnet. Plots are given for different values of DMI.

Paraunitary matrix $T_{\mathrm{I}\mathbf{k}}$ that diagonalizes the Hamiltonian is readily constructed to be

$$T_{\mathrm{I}\mathbf{k}} = \begin{bmatrix}\cosh(\xi_{\mathbf{k}}/2)e^{i\chi_{\mathbf{k}}} & \sinh(\xi_{\mathbf{k}}/2)\\ \sinh(\xi_{\mathbf{k}}/2) & \cosh(\xi_{\mathbf{k}}/2)e^{-i\chi_{\mathbf{k}}}\end{bmatrix}, \qquad (14)$$

where $\sinh(\xi_{\mathbf{k}}) = |\gamma_{\mathbf{k}}|/\sqrt{9-|\gamma_{\mathbf{k}}|^2}$, $\cosh(\xi_{\mathbf{k}}) = 3/\sqrt{9-|\gamma_{\mathbf{k}}|^2}$, and $\gamma_{\mathbf{k}} = |\gamma_{\mathbf{k}}|e^{i\chi_{\mathbf{k}}}$. One can show that the II block described by $\Psi_{\mathrm{II}} = (b_{\mathbf{k}}, a^\dagger_{-\mathbf{k}})^{\mathrm{T}}$ spinor has the paraunitary matrix $T_{\mathrm{II}\mathbf{k}}$ obtained from the $T_{\mathrm{I}\mathbf{k}}$ by setting $\chi_{\mathbf{k}} \to -\chi_{\mathbf{k}}$, and hence has the same O−Berry curvature (see SM for more details). The spin density current can then be written as

$$[\mathbf{J}_{\mathrm{O}}]_\alpha = -\frac{1}{V}\sum_{\mathbf{k}} 2\Omega^{[\mathrm{O}]}_{\alpha\beta}(\mathbf{k})\left[c_1(E_{\mathbf{k}}) - c_1(E_{-\mathbf{k}})\right]\nabla_\beta\chi, \qquad (15)$$

with the diagonal elements of the O−Berry curvature written as

$$\Omega^{[\mathrm{O}]}_{\alpha\beta}(\mathbf{k}) = -\frac{3}{2\left(9-|\gamma_{\mathbf{k}}|^2\right)^{3/2}} \times\left[\left(\partial_\alpha \mathrm{Re}\gamma_{\mathbf{k}}\right)\left(\partial_\beta \mathrm{Im}\gamma_{\mathbf{k}}\right) - \left(\partial_\beta \mathrm{Re}\gamma_{\mathbf{k}}\right)\left(\partial_\alpha \mathrm{Im}\gamma_{\mathbf{k}}\right)\right]. \qquad (16)$$

We observe that the current vanishes if the DMI is zero in the system, in which case $E_{\mathbf{k}} = E_{-\mathbf{k}}$. Note that the O−Berry curvature is independent of the DMI.

Recalling the definition of $\chi(\mathbf{r})$, we define SNE conductivity $\alpha^{\mathrm{s}}_{\alpha\beta}$ as $[\mathbf{J}_{\mathrm{O}}]_\alpha = -\alpha^{\mathrm{s}}_{\alpha\beta}\nabla_\beta T(\mathbf{r})$, and plot its dependence on the temperature - see Fig. 2. We now wish to extract analytic results in the limit of small DMI, $D<J$. There are two different symmetry points, namely $\mathbf{\Gamma}$, and $\mathbf{K}$, $\mathbf{K}'$ points, in the Brillouin zone of magnons the spin current gets major contributions from. Close to $\mathbf{\Gamma} = (0,0)$ point the spectrum is ungapped and linear. We expand all functions close to $\mathbf{\Gamma}$ point to obtain a low temperature, $T<JS$, dependence of the current. See SM for details.

$$\left[(\mathbf{J}_{\mathrm{O}})_x\right]_{\mathbf{\Gamma}} = \frac{5\zeta(5)}{9\sqrt{3}\pi V}\frac{D}{J}\left(\frac{T}{JS}\right)^4\nabla_y T(\mathbf{r}), \qquad (17)$$

where an estimate of Riemann zeta function is $\zeta(5)\approx 1$. At $\mathbf{K} = (0, -4\pi/3)$ and $\mathbf{K}' = (0, +4\pi/3)$ points,

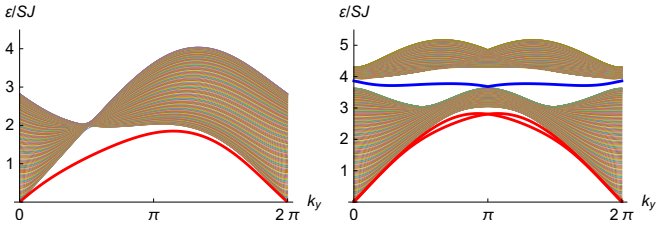

FIG. 3. (Color online) Magnon spectrum of 80 atoms wide strip of honeycomb lattice antiferromagnet. Strip is in $x-$direction, while $y-$direction is assumed infinite. The edges of the system are of the zig-zag type. Left: Single layer with DMI, $D = 0.2J$. Right: Double layer. Protected magnon edge states occur in high energy band gap. Parameters are chosen to be $J' = 1.3J$ and $D = 0.2J$.

the Berry curvature has an absolute value maximum. An analytic estimate of the current contribution from these points at small temperatures $T < JS$, is obtained $[(\mathbf{J}_{\mathrm{O}})_x]_{\mathbf{K}} = \frac{9\sqrt{3}\Lambda^2}{8\pi V}\frac{D}{J}\left(\frac{JS}{T}\right)^2 e^{-\frac{3JS}{T}}\nabla_y T(\mathbf{r})$, where we introduced a high limit cut-off $\Lambda \sim 1$ for k, such that $\sum_{\mathbf{k}} = \frac{\Lambda^2}{4\pi}$. It is straightforward to show that $[(J_{\mathrm{O}})_x]_{\mathbf{\Gamma}} \gg [(J_{\mathrm{O}})_x]_{\mathbf{K}}$ for small temperatures. Both contributions are of the same sign which always results in the same sign of SNE for this model irrespective of the temperature and the strength of DMI.

The Chern number of the magnon band for the single layer honeycomb antiferromagnet is zero (see Fig. 1). As a result we do not observe any protected by the Chern number edge states in the finite strip geometry with a zig-zag edge (see Fig. 3). Nevertheless, we observe an edge state analogous to the zero energy edge state in fermionic model of graphene with a zig-zag or bearded edge. The edge state connects $\mathbf{K}$ and $\mathbf{K}'$ points which have different in sign Berry curvatures. Such edge states do not contribute to the SNE in the finite geometry of a single layer honeycomb antiferromagnet.

Double layer honeycomb antiferromagnet. In another model we consider an antiferromagnet on a double layer honeycomb lattice (see Fig. 1). We again assume nearest neighbor antiferromagnet exchange interaction, second-nearest neighbor DMI, same in both layers, and antiferromagnetic interaction between the layers denoted by J'. With the Neel order being in $z-$direction, we follow the same steps, as in the previous example, and get spectrum of spin waves

$$E^2_{\mathbf{k}\pm}/(SJ)^2 = \lambda^2 - |\gamma_{\mathbf{k}}|^2 + \Delta^2_{\mathbf{k}} - t^2 \pm 2\sqrt{\Delta^2_{\mathbf{k}}(\lambda^2 - |\gamma_{\mathbf{k}}|^2) + t^2|\gamma_{\mathbf{k}}|^2}, \qquad (18)$$

here $\lambda = 3 + t$, where $t = J'/J$. The spectrum and the Berry curvature distribution is shown on Fig. 1. There we observe that the Berry curvature is of the monopole type located at the $\mathbf{M}$ points in the Brillouin zone in contrast to the magnon Haldane-Kane-Mele model [35].

For this model the Chern numbers of the upper and lower bands are $+1$ and -1, respectively, where the topological charge is $1/3$ per $\mathbf{M}$ point. The whole band now contributes in an additive way to SNE which results in a much larger effect. Numerical calculations of the magnon SNE are shown in Fig. 2. To uncover the role of the edge states, we calculate the energy spectrum of a double-layer strip with a zig-zag edge, see Fig. 3. The high-energy edge states here are due to DMI, in contrast to the single-layer model. These edge states are chiral and are protected by the finite Chern number due to the non-trivial topology of the bulk magnons. These edge states are also expected to contribute to SNE conductivity in the finite geometry [24]. The low-energy edge states are of the same nature as in single layer honeycomb antiferromagnet and are not expected to contribute to SNE.

Absence of thermal Hall effect. The thermal Hall coefficient is given by an expression $\kappa_{xy} = -\frac{1}{2T}\sum_{\mathbf{k}}\sum_{n=1}^{2N}[\Omega_{xy}(\mathbf{k})]_{nn}\, c_2\left[(\sigma_3\varepsilon_{\mathbf{k}})_{nn}\right]$, where we defined $c_2(x) = \int_0^x d\eta\, \eta^2 \frac{dg}{d\eta}$. We set $\hat{O} = \sigma_3$ in expression (9), to obtain the Berry curvature of the energy bands $\Omega_{xy}(\mathbf{k}) = i\sigma_3\partial_x T^{\dagger}_{\mathbf{k}}\sigma_3\partial_y T_{\mathbf{k}} - (x \leftrightarrow y)$. For an antiferromagnet on a single layer honeycomb lattice, the energy states are degenerate, corresponding to the two blocks, I and II, with opposite in sign Berry curvatures. The two blocks correspond to two sublattices related either by inversion $\mathcal{I}$ or by time-reversal $\mathcal{T}$ transformations. On the other hand, the double layer antiferromagnet in Fig. 1 is invariant under the global time reversal symmetry if treated as a 2D system since $\mathcal{T}$ followed by interchange of honeycomb layers is a symmetry. Thus, the thermal Hall response considered in [39] vanishes for both models in Fig. 1.

Conclusions. In this paper we theoretically studied magnon mediated SNE in antiferromagnets. We gave a general condition for a current to be a well-defined quantity in an antiferromagnet, and then derived its response to external temperature gradient. We showed that transverse response of this current is defined by a modified Berry curvature. In antiferromagnets with Neel order, SNE can be driven by the Dzyaloshinskii-Moriya interaction and SNE is present even in systems with $\mathcal{TI}$ or global $\mathcal{T}$ symmetries. In both cases the thermal Hall effect is zero while SNE should change sign with the reversal of the Neel vector in the former case but not in the latter case. We also identified the protected edge states with counterpropagating magnon modes, carrying spin but no energy.

Recently we became aware of a paper [49] which discusses SNE in antiferromagnets. The theory presented in the present paper appears to be more general, see results (5), (6), (8), and (9). We also give a solid argument for why the thermal Hall conductivity in studied system should vanish.

Acknowledgements. We gratefully acknowledge useful discussions with K. Belashchenko. This work was sup-

ported primarily by the DOE Early Career Award DE-SC0014189 and in part by NSF under Grants No. Phy-1415600, and No. DMR-1420645.

[1] M. I. Dyakonov, ed., *Spin Physics in Semiconductors* (Springer-Verlag Berlin Heidelberg, 2008).
[2] I. Žutić, J. Fabian, and S. Das Sarma, Rev. Mod. Phys. **76**, 323 (2004).
[3] S. D. Bader and S. S. P. Parkin, Annual Review of Condensed Matter Physics **1**, 71 (2010).
[4] M. I. Dyakonov and V. I. Perel, Phys. Lett. A **35**, 459 (1971).
[5] J. E. Hirsch, Phys. Rev. Lett. **83**, 1834 (1999).
[6] S. Zhang, Phys. Rev. Lett. **85**, 393 (2000).
[7] S. Murakami, N. Nagaosa, and S.-C. Zhang, Science **301**, 1348 (2003).
[8] J. Sinova, D. Culcer, Q. Niu, N. A. Sinitsyn, T. Jungwirth, and A. H. MacDonald, Phys. Rev. Lett. **92**, 126603 (2004).
[9] Y. K. Kato, R. C. Myers, A. C. Gossard, and D. D. Awschalom, Science **306**, 1910 (2004).
[10] S. O. Valenzuela and M. Tinkham, Nature **442**, 176 (2006).
[11] J. Sinova, S. O. Valenzuela, J. Wunderlich, C. H. Back, and T. Jungwirth, Rev. Mod. Phys. **87**, 1213 (2015).
[12] C. L. Kane and E. J. Mele, Phys. Rev. Lett. **95** (2005).
[13] B. A. Bernevig, T. L. Hughes, and S.-C. Zhang, Science **314**, 1757 (2006).
[14] I. M. Miron, K. Garello, G. Gaudin, P.-J. Zermatten, M. V. Costache, S. Auffret, S. Bandiera, B. Rodmacq, A. Schuhl, and P. Gambardella, Nature **476**, 189 (2011).
[15] L. Liu, O. J. Lee, T. J. Gudmundsen, D. C. Ralph, and R. A. Buhrman, Phys. Rev. Lett. **109**, 096602 (2012).
[16] L. Liu, C.-F. Pai, Y. Li, H. W. Tseng, D. C. Ralph, and R. A. Buhrman, Science **336**, 555 (2012).
[17] K.-I. Uchida, S. Takahashi, K. Harii, J. Ieda, W. Koshibae, K. Ando, S. Maekawa, and E. Saitoh, Nature **455**, 778 (2008).
[18] K. Uchida, J. Xiao, H. Adachi, J. Ohe, S. Takahashi, J. Ieda, T. Ota, Y. Kajiwara, H. Umezawa, H. Kawai, et al., Nat. Mater. **9**, 894 (2010).
[19] C. M. Jaworski, J. Yang, S. Mack, D. D. Awschalom, J. P. Heremans, and R. C. Myers, Nat. Mater. **9**, 898 (2010).
[20] X.-L. Qi, Y.-S. Wu, and S.-C. Zhang, Phys. Rev. B **74**, 085308 (2006).
[21] Y. Onose, T. Ideue, H. Katsura, Y. Shiomi, N. Nagaosa, and Y. Tokura, Science **329**, 297 (2010).
[22] T. Ideue, Y. Onose, H. Katsura, Y. Shiomi, S. Ishiwata, N. Nagaosa, and Y. Tokura, Phys. Rev. B **85**, 134411 (2012).
[23] H. Katsura, N. Nagaosa, and P. A. Lee, Phys. Rev. Lett. **104**, 066403 (2010).
[24] R. Matsumoto and S. Murakami, Phys. Rev. Lett. **106**, 197202 (2011).
[25] L. Zhang, J. Ren, J.-S. Wang, and B. Li, Phys. Rev. B **87**, 144101 (2013).
[26] H. Lee, J. H. Han, and P. A. Lee, Phys. Rev. B **91**, 125413 (2015).
[27] M. Hirschberger, R. Chisnell, Y. S. Lee, and N. P. Ong, Phys. Rev. Lett. **115**, 106603 (2015).
[28] R. Shindou, R. Matsumoto, S. Murakami, and J.-i. Ohe, Phys. Rev. B **87**, 174427 (2013).
[29] R. Shindou, J.-i. Ohe, R. Matsumoto, S. Murakami, and E. Saitoh, Phys. Rev. B **87**, 174402 (2013).
[30] A. Mook, J. Henk, and I. Mertig, Phys. Rev. B **90**, 024412 (2014).
[31] A. Mook, J. Henk, and I. Mertig, Phys. Rev. B **89**, 134409 (2014).
[32] A. A. Kovalev and V. Zyuzin, Phys. Rev. B **93**, 161106 (2016).
[33] J. Fransson, A. M. Black-Schaffer, and A. V. Balatsky, Phys. Rev. B **94**, 075401 (2016).
[34] S. A. Owerre, Journal of Applied Physics **120**, 043903 (2016).
[35] S. K. Kim, H. Ochoa, R. Zarzuela, and Y. Tserkovnyak, arXiv preprint arXiv:1603.04827 (2016).
[36] T. Jungwirth, X. Marti, P. Wadley, and J. Wunderlich, Nat. Nanotechnol. **11**, 231 (2016).
[37] Y. Ohnuma, H. Adachi, E. Saitoh, and S. Maekawa, Phys. Rev. B **87**, 014423 (2013).
[38] S. M. Rezende, R. L. Rodríguez-Suárez, and A. Azevedo, Phys. Rev. B **93**, 014425 (2016).
[39] R. Matsumoto, R. Shindou, and S. Murakami, Phys. Rev. B **89**, 054420 (2014).
[40] J. M. Luttinger, Phys. Rev. **135**, 1505 (1964).
[41] G. Tatara, Phys. Rev. B **92**, 064405 (2015).
[42] A. A. Tsirlin, O. Janson, and H. Rosner, Phys. Rev. B **82**, 144416 (2010).
[43] X. Liu, T. Berlijn, W.-G. Yin, W. Ku, A. Tsvelik, Y.-J. Kim, H. Gretarsson, Y. Singh, P. Gegenwart, and J. P. Hill, Phys. Rev. B **83**, 220403 (2011).
[44] S. Lee, S. Choi, J. Kim, H. Sim, C. Won, S. Lee, S. A. Kim, N. Hur, and J.-G. Park, J. Phys.: Condens. Matter. **24**, 456004 (2012).
[45] Y. Singh, S. Manni, J. Reuther, T. Berlijn, R. Thomale, W. Ku, S. Trebst, and P. Gegenwart, Phys. Rev. Lett. **108**, 127203 (2012).
[46] S. K. Choi, R. Coldea, A. N. Kolmogorov, T. Lancaster, I. I. Mazin, S. J. Blundell, P. G. Radaelli, Y. Singh, P. Gegenwart, K. R. Choi, et al., Phys. Rev. Lett. **108**, 127204 (2012).
[47] A. Auerbach, *Interacting Electrons and Quantum Magnetism* (Springer New York, 1994).
[48] L. Smrcka and P. Streda, J. Phys. C **10**, 2153 (1977).
[49] R. Cheng, S. Okamoto, and D. Xiao, arXiv:1606.01952 (2016).